Lehrstuhl für Bildverarbeitung
Institute of Imaging & Computer Vision

Automatic Calibration of a Scanner-Based Laser Welding System

Nicolaj C. Stache and André Stollenwerk and Jens Gedicke and Alexander Olowinsky and Achim Knepper and Til Aach
Institute of Imaging and Computer Vision
RWTH Aachen University, 52056 Aachen, Germany
tel: +49 241 80 27860, fax: +49 241 80 22200
web: www.lfb.rwth-aachen.de

in: International Congress on the Applications of Lasers and Electro-Optics (ICALEO). See also BibTeX entry below.

BibTeX:

```
@inproceedings{STA07c,
  author       = {Nicolaj~C.~Stache and Andr{\'e}~Stollenwerk and Jens~Gedicke and Alexander~Olowinsky
                  and Achim~Knepper and Til~Aach},
  title        = {Automatic Calibration of a Scanner-Based Laser Welding System},
  booktitle    = {International Congress on the Applications of Lasers and Electro-Optics (ICALEO)},
  organization = {Laser Institute of America},
  publisher    = {Laser Institute of America},
  address      = {Orlando, Florida, USA},
  month        = {Oct.\ 29--Nov.\ 1},
  year         = {2007},
  pages        = {223--229}}
```

AUTOMATIC CALIBRATION OF A SCANNER-BASED LASER WELDING SYSTEM

Paper (#M804)

Nicolaj C. Stache[1], André Stollenwerk[1], Jens Gedicke[2], Alexander Olowinsky[2], Achim Knepper[1], and Til Aach[1]

[1] Institute of Imaging and Computer Vision, RWTH Aachen University, D-52056 Aachen, Germany
[2] Fraunhofer Institute for Laser Technology, Steinbachstr. 15, 52074 Aachen, Germany

Abstract

In precision engineering scanners are widely used for laser beam positioning. Equipped with cameras, scanners enable process monitoring or even position recognition of the parts to be welded.

To allow precise welding or position recognition, it is essential to calibrate a welding system. Instead of calibrating the whole system, most approaches only help to adjust the laser beam position. Consequently, the varying lateral offset between the laser's focus point and the camera's field of view, due to chromatic aberration of the scanner optics, cannot be compensated. Furthermore, these approaches require manual microscopic measurement of weld seams, which comes along with several downsides.

This paper proposes two techniques for automatic calibration without these downsides by use of the system-incorporated camera. The first technique is the calibration at laser wavelength. To this end, the system automatically creates laser spots, evaluates their positions and possible offsets and finally fits an affine model for compensation. The second technique is based on a specially coded test pattern, which is used for calibration at camera wavelengths.

Experimental results confirm the accuracy of the calibration obtained.

Introduction

Galvanometer scanners (galvo scanners) have evolved into a common tool for laser beam positioning due to, among others, the high achievable speed combined with exceptionally high accuracy. These properties permit the use of scanners in precision engineering industry, where high demands on accuracy and speed are imposed, e.g., in mass production of filters.

The capabilities of a plain scanner based welding system can be considerably extended by a high speed CMOS camera, which is connected to the scanner. As already proven in setups without scanners, cameras are well suited for coaxial inline process monitoring [3, 1], see Figure 1.

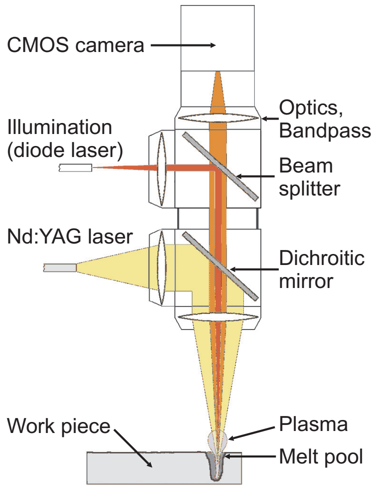

Figure 1: CPC-System (Coaxial Process Control) [3]

Equipped with a diode laser for illumination at a specific wavelength, as shown in Figure 1, such setups allow image acquisition of the keyhole without being disturbed by plasma radiation. Thus, highly accurate measurements of the melt can be conducted, which is introduced in [5, 6]. In case of extending this setup with a scanner, the entire system has to be calibrated, as described below in detail.

Besides process monitoring, a camera-equipped scanner setup facilitates image acquisition of the parts to be welded in order to measure their positions. With these measurements, the welding system does not require exactly positioned parts – it automatically determines the positions and adjusts the laser correspondingly.

Such a system, which we concentrate on in this contribution, is sketched in Figure 2. As illustrated, the scanner (Scanlab Hurryscan 25) is equipped with a telecentric f-theta optics (Sill S4LFT0080/126) and a LED ring illumination (dominant wavelength =

630 nm) to illuminate the work piece. The laser used for welding is a pulsed Trumpf HL62P Nd:YAG laser, and the camera is of type Photonfocus MV-D1024-160 with a 1 mega pixel sensor. The laser partly shares the optical path with the camera, which is realized using a dichroit. As indicated, the system can be extended with further modules, e.g., a diode laser for additional illumination, which provides the functionality of the CPC-system in Figure 1 and enables melt pool monitoring, as mentioned above.

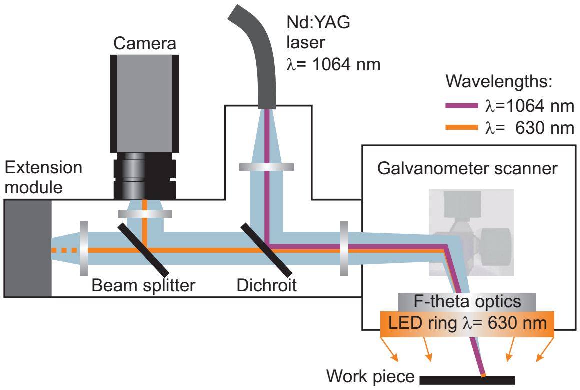

Figure 2: Scanner system with camera for position estimation

The objective of this contribution is to address the problem which always arises when beams of different wavelengths pass through the f-theta optics of a scanner: Due to chromatic aberration of the optics, the beams will be refracted differently (except for central beams).

In case of position estimation, the camera will therefore capture a different center of view than the laser's lateral focus position. In Figure 3 (b) this lateral offset is sketched, which is caused by different refraction of two rays with different wavelengths due to chromatic aberration. Only in exact center position, see Figure 3 (a), when both optical paths remain unchanged, the laser focus point will exactly match the camera's reference point – except for the different focus position in axial direction. Unlike this axial offset, which can be compensated with an additional optics in front of the camera, compensation of the lateral offset requires expensive achromatic correction of the f-theta lens.

Therefore, we describe a much cheaper and more flexible approach, which is based on measuring the lateral offsets and fitting a model to these. More precisely, we propose a calibration of the system for laser and camera wavelengths.

In contrast to existing calibration methods, which require to place weldings on a target and determine the position manually with a microscope, our approach makes use of the system-internal components and thus allows to perform calibration without external examination of a target. Hence, error-prone and tedious manual interaction is avoided.

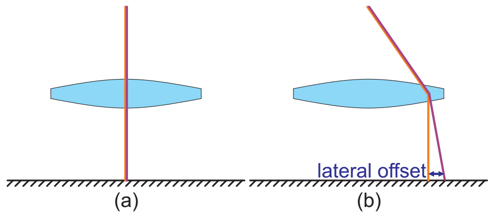

Figure 3: Offset caused by chromatic aberration of the lens

To this end, we develop two calibration techniques. The first one is based on creating laser spots and detecting them, while the second one works with a specially designed coded test pattern to estimate the camera's field of view position exactly.

The organization of the paper follows the order of the mentioned calibration methods. In addition, experimental results of the achievable accuracy are presented. We conclude with a discussion and an outlook on future work.

System Calibration

From the point of the system in Figure 2, calibration uses three different coordinate systems, which have to be related to each other by appropriate mapping functions. Figure 4 gives an overview about these coordinate systems and the corresponding mapping functions, indicated by ①, ②, and ③.

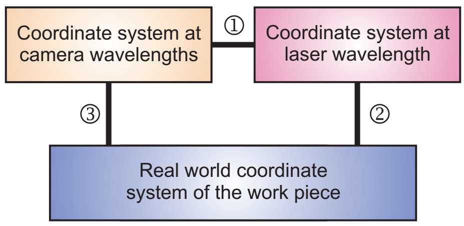

Figure 4: Relations between the three coordinate systems to be calibrated

The first issue we address is to find a mapping between the camera's coordinate system and the laser's coordinate system. In many cases, this might be sufficient for calibrating the entire system, since the scanner is usually already calibrated for a given laser wavelength, as the mapping function denoted by ② has already been determined by the manufacturer.

In the considered Scanlab Hurryscan 25 system, a basic mapping function is implemented in the scanner control hardware and cannot be deactivated by the user. Consequently, the estimation of the "original" mapping function ② is not treated in this contribution. Nevertheless the calibration of function ② might be helpful, e.g., when the original calibration of the manufacturer is insufficient or when different laser wavelengths should be processed with the scanner. We thus develop a technique, which can be used in such cases for calibration on the basis of the hardware implemented mapping function in only two calibration steps.

The mapping functions directly estimated in this paper are function ①, which is the relation of the system at laser wavelength to camera wavelengths and function ③, which relates the real world coordinates to the acquired images. As it is intuitively clear in Figure 4, mapping function ② can be easily inferred in two steps by estimating ① and ③ and subtracting them. Even if function ② is assumed to be known with adequate accuracy and thus the system has not to be recalibrated entirely, the two different approaches we describe, offer the opportunity to choose the optimal procedure for estimating function ①. Hence, the calibration approach can be chosen depending on the requirements of the individual application. Furthermore, an evaluation of both approaches allows to check the consistency of the resulting calibrations.

Calibration of Laser and Camera (Mapping ①)

Our approach consists of four steps. First, laser spots have to be created on a test target at positions which are defined in the coordinate system of the laser. Second, without any move of the scanner, images of the laser spots are acquired by the system's coaxial camera. Third, the positions of these spots have to be detected in the images. Finally, the calibration model is determined with the offset vectors between real and nominal positions.

To enable automatic spot detection with high accuracy, it is important to create sharply rimmed round spots with high contrast to the background. Therefore, the material of the test target has to be carefully chosen to obtain optimal results. We chose thermal paper, mounted on an acrylic glass target because it optimally satisfies the mentioned conditions. Of course, the power of the laser and the pulse width have to be adapted to this medium in order to prevent the laser from uncontrollably burning the paper and not just blackening it. Once adapted (in our case: pulse energy = 0.15 J, pulse width = 5 ms, irradiation power = 30 W), the welding system creates 9 x 9 spots in an equally spaced grid (3 mm grid width) on the thermal paper. At each position, the camera acquires an image.

Figure 5 shows two such images acquired with the system's camera. Figure 5 (b) was acquired in the periphery of the scan field and Figure 5 (a) shows the image in the scan field's center. In comparison to image (a), where the laser spot is at the expected position (marked by the yellow circle), the spot in image (b) is unexpectedly located at a different position. This is due to different refraction of camera and laser wavelength by the f-theta optics. As already indicated in Figure 3, only in center position of the scanner the two optical paths remain unaffected – see Figure 5 (a).

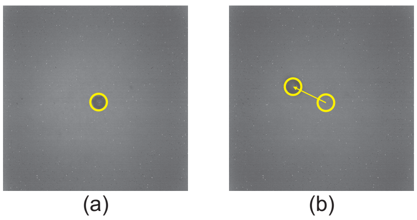

Figure 5: Laser spots on thermal paper (image size: 7.06 x 7.06 mm²); (a) at the scan field's center (x,y = 0 mm, 0 mm), (b) at the periphery of the scan field (x,y = –12 mm, –12 mm).

Subsequent to image acquisition we automatically detect the position for each of the 9 x 9 spots and compute the offsets to fit an affine calibration model with six degrees of freedom. For position detection the algorithm first segments the dark points from background via an adapted threshold, then it rejects all points which are not of reasonable size to gain greater stability against errors. Finally, it fits a circle model to the remaining points to exactly determine the sought positions and the offset vectors to nominal positions with high accuracy.

To robustly fit the affine model with the thus determined vectors, a first fit via least mean squares regression is performed. Then, the deviation of each offset vector to the model is calculated and a second fit is conducted to a selection of vectors which are assumed to be undisturbed. This selection is made by computing the median of the differences between the vectors and the previously estimated model. Only those vectors are selected as undisturbed which lie in a small threshold band around this median. Thus, the robustness to gross outliers is significantly increased.

Results of the Calibration (Mapping ①)

Figure 6 displays the results of the measurements carried out. The blue arrows visualize the measured lateral offsets, as already shown in Figure 5, for the different 9 x 9 field of view positions.

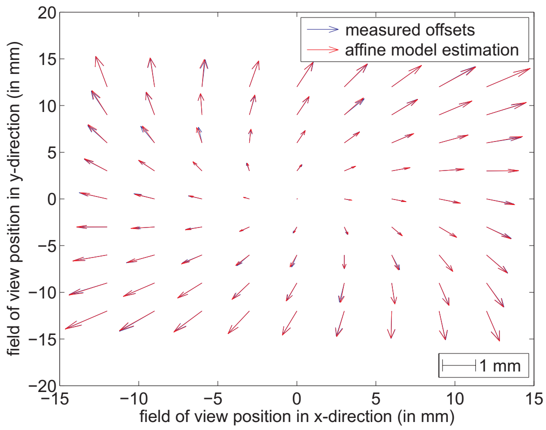

Figure 6: Offset vectors at 9 x 9 positions, measured and modelled with an affine model (6 degrees of freedom). The maximum offset (longest arrow) is 1.26 mm.

Not surprisingly, the arrow in center position is of length zero and the lengths increase linearly with the distances to the center [4]. In addition, there is a slight rotation, which may be due to inaccuracies in camera adjustment. The red arrows represent the offsets, estimated with the affine model, fitted robustly to the blue arrows as described before. In almost all measurements, the red arrow covers the blue, which indicates that the model has well adapted to the measurements. To make sure that the estimation error is non-systematic and to give an impression about the values of deviation, Figure 7 visualizes the difference vectors between the estimated and the measured values. The figures, printed next to the arrows, symbolize the Euclidean lengths of these arrows in µm.

As Figure 7 shows, adjacent vectors tend to differ significantly, which indicates that the deviations are due to typical noise in the measurements. The mean deviation, determined with a test dataset with 18 randomly spread laser spots is approximately 20 µm which corresponds to 3 pixels of the camera's sensor. However, this is less than 1/60 of the maximum offset before calibration.

The accuracy of the model may be increased by improving the camera's optics which is up to now a single lens which exhibits strong vignetting and blurring in the image's periphery. In addition, despite of using thermal paper to ensure sharply rimmed spots, it is still challenging to decide where the exact spot position is, as illustrated in Figure 8.

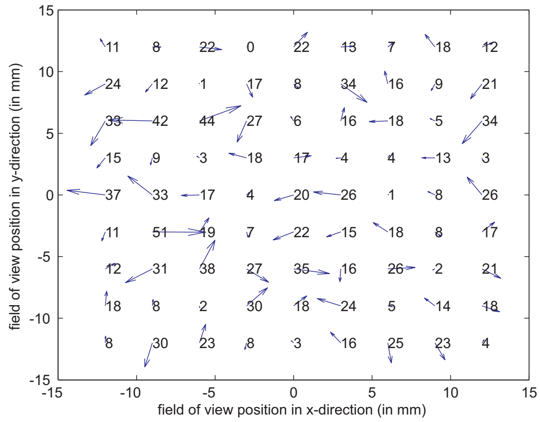

Figure 7: Visualization of the difference vectors between "measured offsets" and "affine model estimation". The figures represent the Euclidean lengths of the vectors in µm.

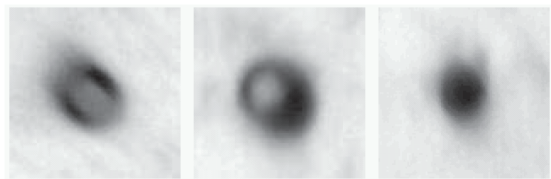

(a) (b) (c)

Figure 8: Challenging laser spots

Calibration of Camera Coordinates to Real World Coordinates (Mapping ③)

This section describes the calibration of the camera to the real world coordinate system of the work piece, which is denoted as mapping ③ in Figure 4. In order to conduct this calibration, a reference in the real world coordinate system is needed, which exactly allows to identify the position in images taken of it. Consequently, the field of view position can be located in the real world coordinate system, which, in turn, is used to determine the calibration.

The procedure of calibration is as follows: First, the mentioned reference target is placed in the work piece's plane. Second, the scanner moves to the 9 x 9 previously determined grid positions like in the calibration described in the previous section. At each position the camera acquires an image of the target.

Then, the position (in work piece's coordinates) of the center point in the image is determined via the reference information on the target. Thus, the position of the camera's field of view in real world coordinates can be exactly determined and furthermore related to the 9 x 9 grid positions used for scanner positioning. If the scanner is accurately calibrated by the manufacturer, these nominal grid positions are equivalent to the real world coordinates of possible laser spots on the work piece. Therefore, the calibration result would be identical with the result of laser–camera calibration, which is denoted by mapping ①. This is why the calibration with the reference target may be seen as an alternative to the procedure via laser spots on thermal paper. However, in case of non-ideal calibration of the manufacturer, the obtained result would be distorted by the increasing influence of compensation in mapping ②.

Calibration Pattern

Paramount for the sought calibration in this section is the design of the reference target or calibration pattern. The main idea behind our target is the design of an optimally camera-readable pattern, which encodes the precise position information in the work piece's plane.

Commonly used for camera calibration purposes are checkerboard patterns. Although these patterns are well suited to calibration of static cameras, the scanner system requires accurate calibration of a moving camera's field of view. Hence, a conventional checkerboard pattern is not applicable, since it just allows accurate detection of moves within one checkerboard period, viz., a checkerboard may exhibit identical images at different field of view positions, due to periodicity.

Therefore, we individualize each black field of the checkerboard pattern as shown in Figure 9.

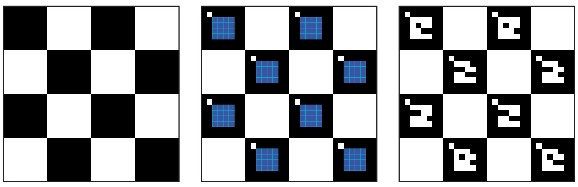

(a) (b) (c)

Figure 9: Composition of the calibration pattern

To this end, the black fields are subdivided into 4 x 4 blocks, which are used for binary encoding the position of each black field individually, see Figure 9 (b). More precisely, each black field thus contains a unique identification code which is implemented via a Gray-code using the 4 x 4 blocks as bits. With this camera readable identification code, see Figure 9 (c) and the knowledge of the target's composition, the position of each black field and thus the camera's field of view position can be reconstructed.

However, the accuracy of the position estimation can be further increased by additional use of the white checkerboard fields. The easily segmentable white fields allow the computation of the centroids with sub pixel accuracy. As a result, the centroids of the white fields allow estimating the position within one period of the checkerboard pattern. Combined with the identification code, which provides the position in the periodicity of the checkerboard, the overall position can be accurately determined.

Detection Algorithm

The software for automatic position estimation via the calibration pattern works as follows: In a first step, the gray values in the acquired images are adjusted for optimal processing. After this pre-processing step, the white blocks of the checkerboard are sought to infer the positions of the black fields and decode the incorporated information later on. This succession is reasonable because it is much easier to estimate the position of the unchanged and homogeneous white fields than the individualized black fields.

In order to estimate the positions of the white fields, the image's pixels are classified into black and white via a locally adapted threshold, determined with Otsu's algorithm [2]. In this classified result, called mask image, the area of adjacent white pixels is evaluated and, with this criterion, the white checkerboard fields are selected. Subsequent to this step, the centroids of the white fields are computed and hence, the center of the encoded black fields is determined with sub pixel accuracy. Finally, with the information of the center and the centroids of surrounding white fields, which is used to adapt to possible rotation of the acquired image, the information can be decoded. To this end, the mean gray values are sampled in the original image at the positions where the 4 x 4 blocks are assumed to be. However, first of all, the white marker in the top left corner of each black field, see Figure 9 (b-c), is evaluated to determine the correct orientation of the pattern. After this step and sampling of the 4 x 4 gray values of the blocks, a robust classification of each block has to be conducted, viz., it has to be decided whether the block is black or white. Therefore, the gray values of the white checkerboard patterns are used to obtain a gray value as initial white reference and the black rims of the black fields are used for initial black reference. After obtaining these values, an iterative classification starts to classify each individual block in three classes, i.e., white, black, and indifferent. The indifferent blocks are subject to further classification iterations, which consider more prior information, i.e., the gray values of indifferent blocks are now compared with gray values of adjacent blocks, which have already been classified into black or white. This iterative procedure continues until each block is clearly classified. Thus, the identification code can be decoded even in blurred or noisy images, see Figure 10.

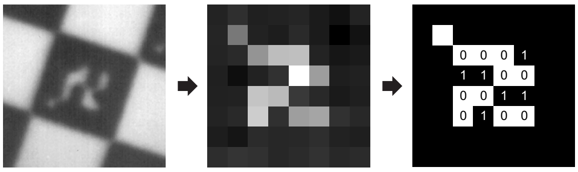

Figure 10: Decoding of the identification code of a black filed (Gray-code 0001110000110100 → 6104 decimal value). (a): detail of the checkerboard pattern, acquired with the camera, (b): sampled gray values, (c): classification result.

Results of the Calibration (Mapping ③)

Since the results for mapping ③ of the manufacturer-calibrated scanner we use should rather look like in Figure 6, we concentrate here on evaluating the accuracy of position detection via the test pattern.

Therefore, an experiment has been conducted where the calibration pattern is mounted on a translation stage. With this experimental setup, the pattern is shifted in steps of 1 µm which are additionally measured with a mechanical dial indicator. At each position a camera setup, similar to the scanner system, acquires ten images of the pattern. Due to a pixel size of 6.73 µm, the shifts thus generate sub pixel shifts in the images.

This workflow is executed for 21 steps of 1 µm. Figure 11 visualizes the estimated offset depending on the given offset. The small deviations from the plotted line to the ideal diagonal are mainly due to the inaccuracies of the given offset, since the translation stage requires manual adjustment of the 1 µm shifts. However, despite of these deviations, the estimated position deviates less than 0.5 µm from the assumed given position. The small blue horizontal bars indicate the standard deviation within the ten measurements at each position, whose mean in 21 x 10 measurements is 0.0977 µm or 0.0145 pixel.

In conclusion, the experimental setup confirms that the calibration pattern enables position estimation with sub pixel accuracy (1 µm ≈ 0.15 pixel) and offset detection far less than 1 µm. It thus exceeds the accuracy of the preceding calibration method, provided that the calibration pattern is of adequate precision.

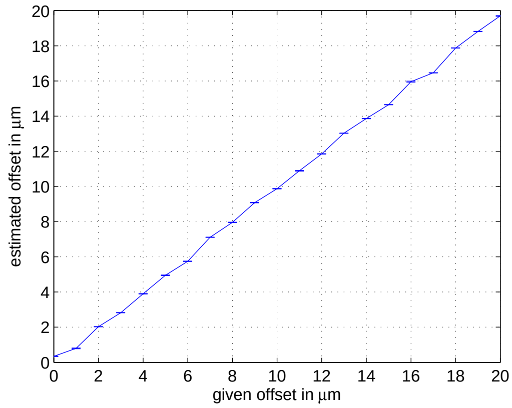

Figure 11: Experimental result of the accuracy in position detection with the calibration pattern

Conclusions and Outlook

In near future, an increasing amount of scanner based welding systems will be equipped with cameras in order to coaxially monitor the welding process or to perform position recognition. In both cases radiations of different wavelengths usually pass through the scanner and its optics. Due to chromatic aberrations in the optics, beams of different wavelengths refract differently and thus a lateral offset appears, which makes position estimation and process control more difficult.

However, an achromatically corrected optics would ameliorate this problem but suffers from high costs of a appropriately corrected optics. Furthermore, flexibility in changing the wavelengths may be affected.

This contribution thus describes two ways for calibrating the optics of such a system without tedious manual interaction and without using expensive additional components. In case of a system already calibrated for one wavelength, the calibration method can be freely chosen depending on the system to be calibrated, since the two techniques should yield the same calibration models. The accuracy of the resulting calibration has proved to be sufficient to permit further image processing steps such as image stitching or position estimation.

Our future work will be on the improvement of the calibration's accuracy, e.g., by examining a larger amount of laser spots. Another aspect will be a redesign of the calibration pattern with a more sophisticated encoding scheme in order to enhance robustness to decoding errors. Last but not least, calibration will be tried for use in further scanner based welding systems with different wavelengths in order to accomplish process monitoring and we will try to calibrate scanner systems without pre-installed manufacturer's calibration.

Acknowledgments

This work is funded by the collaborative research project "INTAKT" in the funding program "InnoNet" from the German Federal Ministry of Economics and Technology (BMWi) with VDI/VDE-IT. The authors gratefully acknowledge this support as well as the active cooperation of all project partners.

References

[1] Aaldering, B. J., Aarts, R. G. K. M., Jonker, J. B., Meijer, J. (2005) Experimental Observation of the Laser Keyhole Welding Process of AA5182, ICALEO, Miami, Florida, USA, 832–836.

[2] Otsu, N. (1979) A threshold selection method from gray level histograms, IEEE Transactions on Systems, Man, and Cybernetics, vol. 9, pp. 62–66.

[3] Regaard, B., Kaierle, S., Schulz, W., Moalem, A. (2005) Advantages of Coaxial External Illumination for Monitoring and Control of Laser Materials Processing, ICALEO, Miami, Florida, USA, 915–919.

[4] Smith, W. J. (2000) Modern Optical Engineering, 3rd ed., McGraw-Hill, New York, 61–89.

[5] Stache, N. C., Zimmer, H., Gedicke, J., Olowinsky, A., Aach, T. (2007) Robust High-Speed Melt Pool Measurements for Laser Welding with Sputter Detection Capability, Proceedings of the 29th Annual Symposium of the German Association for Pattern Recognition, Heidelberg, Germany.

[6] Stache, N. C., Zimmer, H. (2007) Robust Circle Fitting in Industrial Vision for Process Control of Laser Welding, Proceedings of the 11th International Student Conference on Electrical Engineering POSTER 2007, Prague, Czech Republic.

Meet the Author

Nicolaj C. Stache received his diploma degree in Electrical Engineering from RWTH Aachen University, Germany, in 2005. He is now working towards his doctoral degree at the Institute of Imaging and Computer Vision, RWTH Aachen University. His research interests are feature extraction, orientation estimation, and industrial applications such as position recognition. Currently, he concentrates on video-guided laser welding processes.